12-*O*-tetradecanoylphorbol-13-acetate reduces activation of hepatic stellate cells by inhibiting the Hippo pathway transcriptional coactivator YAP

Chang Wan Kim

The Graduate School
Yonsei University
Department of Medicine

12-*O*-tetradecanoylphorbol-13-acetate reduces activation of hepatic stellate cells by inhibiting the Hippo pathway transcriptional coactivator YAP

A Dissertation
Submitted to the Department of Medicine
and the Graduate School of Yonsei University
in partial fulfillment of the
requirements for the degree of
Doctor of Philosophy in Medical Science

Chang Wan Kim

December 2022

This certifies that the dissertation
of Chang Wan Kim is approved.

_____

Thesis Supervisor: Il Hwan Park, M.D., Ph.D.

_____

Thesis Committee Member: Hoon Ryu, M.D., Ph.D.

_____

Thesis Committee Member: Pil Young Jung, M.D., Ph.D.

_____

Thesis Committee Member: Chun Sung Byun, M.D., Ph.D.

_____

Thesis Committee Member: Young Woo Eom, Ph.D.

The Graduate School
Yonsei University
December 2022

감사의 글

이 논문이 나오기까지 바쁘신 와중에도 아낌없는 지도를 해 주신 박일환 교수님께 깊이 감사드립니다. 또한 소중한 시간을 내어 지도해 주신 류훈 교수님, 정필영 교수님, 변천성 교수님, 엄영우 교수님께 감사드립니다. 교수님들의 도움과 지도가 없었으면 학위를 시작하고 마치는 것이 어려웠을 것입니다. 진심으로 감사드립니다.

그리고, 항상 연구와 진료 등 모든 분야에서 물심양면으로 지원을 아끼지 않는 흉부외과 이상헌 선생님께 감사의 말씀은 전합니다.

마지막으로 부족한 남편을 항상 믿고 바라봐 주며 격려와 응원을 아끼지 않은 사랑하는 아내 이정민에게도 고마움과 사랑을 전합니다.

2022 년 12 월

김 창 완 올림

Index

Figure index · iii

Abstract · iv

I. Introduction · 1

II. Materials and methods · 4

1. Materials · 4

2. Cell culture · 5

3. MTT assay · 5

4. qPCR · 6

5. Immunoblotting analysis · 8

6. Immunocytochemical analysis · 8

7. Cell cycle analysis · 9

8. Statistical analysis · 9

III. Results · 11

1.TPA-induced inhibition of activation of hepatic stellate cells · · · · · · · · 13

2. TPA-induced phosphorylation of PKCδ and YAP in HSCs · · · · · · · · · · 14

3. Roles of PKCδ and YAP in HSC activation · · · · · · · · · · · · · · · 19

IV. Discussion · 24

References · 26

Abstract in Korean · 40

Figure Index

Fig. 1. Inhibition of growth and expression of α-SMA in TPA-treated LX-2 cells. · 13

Fig. 2. Phosphorylation of PKCs in TPA-treated LX-2 cells. · · · · · · · · · · · 16

Fig. 3. Phosphorylation and cellular distribution of YAP in TPA-treated LX-2 cells. · 17

Fig. 4. Effects of the pan-PKC inhibitor Gö 6983 on the proliferation and fibrosis of TPA-treated LX-2 cells. · 20

Fig. 5. Phosphorylation and cellular distribution of YAP in LX-2 cells treated with TPA or Gö 6983 or both. · 22

ABSTRACT

12-*O*-tetradecanoylphorbol-13-acetate reduces activation of hepatic stellate cells by inhibiting the Hippo pathway transcriptional coactivator YAP

Chang Wan Kim

Dept. of Medicine

The Graduate School

Yonsei University

Although protein kinase C (PKC) regulates various biological activities, including cell proliferation, differentiation, migration, tissue remodeling, gene expression, and cell death, the antifibrotic effect of PKC in myofibroblasts is not fully understood. We investigated whether 12-O-tetradecanoylphorbol-13-acetate (TPA), a PKC activator, reduced the activation of hepatic stellate cells (HSCs) and explored the involvement of the Hippo pathway transcriptional coactivator YAP. We analyzed the effect of TPA on the proliferation and expression of α-smooth muscle actin (SMA) in the LX-2 HSC line. We also analyzed the phosphorylation of the Hippo path-way molecules YAP and LATS1, and investigated YAP nuclear translocation. We examined whether Gö 6983, a pan-PKC inhibitor, restored the TPA-inhibited activities of HSCs. Administration of TPA decreased

the growth rate of LX-2 cells and inhibited the expression of α-SMA and collagen type I alpha 1 (COL1A1). In addition, TPA induced phosphorylation of PKCδ, LATS1, and YAP and inhibited the nuclear translocation of YAP compared with the control. These TPA-induced phenomena were mostly ameliorated by Gö 6983. Our results indicate that PKCδ exerts an antifibrotic effect by inhibiting the Hippo pathway in HSCs. Therefore, PKCδ and YAP can be used as therapeutic targets for the treatment of fibrotic diseases.

Key words: 12-O-tetradecanoylphorbol-13-acetate; hepatic stellate cell; protein kinase Cδ; Yes-associated protein 1

I. Introduction

Hepatic stellate cells (HSCs), which are liver resident fibroblasts, are located in the space of Disse between hepatocytes and sinusoidal endothelial cells and constitute 5–8 % of total liver resident cells [1,2]. Quiescent HSCs in the normal liver play an important role in supporting liver development and regeneration, vitamin A storage, intracellular lipid droplet storage, immunoregulation, and liver hemodynamic homeostasis [3,4]. Liver injury stimulates the transdifferentiation of quiescent into activated HSCs. During activation, the properties of HSCs change, including their proliferation, ECM production, migration towards chemokines, contraction, and loss of lipid droplets, ultimately promoting hepatic fibrosis [5-10]. As the quantity of activated HSCs is known to correlate with fibrosis severity [11,12], controlling the activity of HSCs is considered essential for the treatment of liver fibrosis.

Protein kinase C (PKC) is a group of serine/threonine protein kinases that play important roles in various biological functions, including cell proliferation, differentiation, migration, gene transcription and translation, and apoptosis [13-16]. PKC isoforms are grouped into 4 classes: conventional (cPKCs; α, βI, βII, and γ), novel (nPKCs; δ, ε, η, and θ), atypical (aPKCs; ζ, λ/ι), and PKCμ (a form between novel and atypical isoforms) isoforms [17]. Of note, cPKCs are Ca2+- and diacylglycerol-dependent, nPKCs are Ca2+-independent and diacylglycerol-dependent, whereas aPKCs are Ca2+- and diacylglycerol-

independent. The expression of PKC isoforms is known to differ not only between species, but also be-tween normal and disease states in the same organism [18]. Most studies have suggested that PKCs are associated with the malignant transformation of cells, including breast [19], lung, and gastric carcinoma [20], as well as with the promotion of fibrosis [21-23].

The Yes-associated protein 1 (YAP)/transcriptional coactivator with PDZ-binding motif (TAZ) signaling has been linked to the pathophysiology of fibrosis. Interestingly, aberrant activation of YAP/TAZ has been observed in human fibrotic tissues (i.e., lung, kidney, skin, and liver), animal models of fibrosis (i.e., bleomycin-induced lung or skin fibrosis, diabetic nephropathy, and non-alcoholic steatohepatitis), and various cultured cells (i.e., fibroblasts, epithelial cells, keratinocytes, and hepatocytes) [24-35]. Activation of YAP, which is represented by its translocation to the nucleus, is a critical driver of hepatic stellate cell activation, leading to α-SMA expression [36,37]. The phosphorylation of YAP at Ser-127 promotes its cytoplasmic retention, whereas phosphorylation at Ser-397 induces its degradation [38].

12-O-tetradecanoylphorbol 13-acetate (TPA) is used as a cPKC or nPKC activator be-cause it can substitute diacylglycerol by directly binding to the C1 domain, leading to PKC activation. TPA is broadly used as an immune cell stimulator and for understanding the cell-specific function of PKC isoforms. TPA can increase the cell proliferation of malignant cells in several types of tumors and thus acts as a promotor for melanoma, breast cancer, oral cancer, and skin carcinogenesis [39-41]. In contrast, treatment with TPA decreases the

proliferation capacity of lymphoma and liver cancer cells [42-44]. Many studies have reported that PKCs promote fibrosis [45-47]; however, TPA was recently reported to weaken the proliferation and transdifferentiation of cardiac fibroblasts through cPKC and nPKC [48]. In addition, we found that the proliferation of LX-2 hepatic stellate cells and expression of α-SMA were both suppressed when LX-2 cells were cocultured with TPA-induced macrophages from monocytic THP-1 cells.

Based on these findings, we hypothesized that PKC activity could alleviate liver fibrosis. Hence, we examined whether induction of PKC activity in TPA-treated LX-2 hepatic stellate cells alleviates fibrosis in vitro. To this end, we investigated whether TPA suppresses the proliferation of LX-2 cells and expression of α-SMA and whether the Hippo pathway transcriptional coactivators YAP/TAZ are involved in the regulation of this activity. Through comprehensive analysis, we aimed to evaluate whether the induction of PKC activity can be used as a therapeutic approach for the treatment of liver fibrosis.

II. Materials and methods

1. Materials

TPA and methylthiazolyldiphenyl tetrazolium bromide (MTT) were obtained from Sigma-Aldrich (St. Louis, MO, USA), while TGF-β was purchased from R&D Systems (Minneapolis, MN, USA). Antibodies against α-SMA (ab7817) were from Abcam (Cambridge, UK), antibodies against PKCδ (sc396), YAP (sc101199), Lats1 (sc398560), and GAPDH (sc47724) were from Santa Cruz Biotechnology (Santa Cruz, CA, USA), while antibodies against PKCs (phospho-PKC antibody sampler kit, 9921T), COL1A1 (39952S), pLats1 (8654S), pYAP(4911S), and horseradish peroxidase-conjugated secondary antibodies (7074S and 7076S) were obtained from Cell Signaling Technology (Danvers, MA, USA). ProLong™ Gold Antifade Mountant with DAPI (4',6-diamidino-2-phenylindole; P36930) was purchased from Invitrogen (Waltham, MA, USA), while the pan-PKC inhibitor Gö 6983 (HY-13689) was acquired from MedChemExpress (Princeton, NJ, USA). All other materials were purchased from Sigma-Aldrich unless otherwise indicated

2. Cell culture

The LX-2 human HSC line was purchased from Millipore (Burlington, MA, USA). LX-2 cells were maintained in Dulbecco's modified Eagle medium (DMEM, Gibco BRL, Rockville, MD, USA) supplemented with 3 % fetal bovine serum (FBS, Gibco BRL) and penicillin/streptomycin (Gibco BRL) at 37 °C and 5 % CO2. For experiments, LX-2 cells were seeded for 24 h, and treated with TPA for an additional 48 h. Cells were exposed to Gö 6983 20 min prior to TPA treatment

3. MTT assay

Cells were seeded at a density of 1×10^4 cells/cm2 in 96-well plates and cultured for 24 h and treated with TPA (0.01 to 100 nM) and then cultured for an additional 48 h. Then, Gö 6983 (1 μM) was added to LX-2 cells 20 min before TPA treatment to inhibit the activation of PKCs. MTT dissolved in phosphate-buffered saline (PBS) was added to each well (final concentration: 5 mg/mL), and cells were further incubated at 37 °C for 2 h. MTT formazan was dissolved in 100 μL dimethyl sulfoxide following incubation for an additional 15 min with shaking. Subsequently, the optical density of each well at 570 nm was measured using a microplate reader (Molecular Devices; San Jose, CA, USA

4. qPCR

Total RNA was extracted using TRIzol reagent (Gibco BRL) according to the manufacturer's instructions. cDNA was synthesized from 1 μg total RNA using the Verso cDNA synthesis kit (Thermo Fisher Scientific, Waltham, MA, USA). The expression of α-*SMA, COL1A1, COL3A1,* and *GAPDH* was evaluated using the respective sense and antisense primers (Table 1). The reaction mixture (10 μL) included cDNA, primer pairs, and SYBR Green PCR Master Mix (Applied Biosystems, Dublin, Ireland), and PCR was con-ducted using a QuantStudio 6 Flex Real-time PCR System (Thermo Fisher Scientific). All qPCR reactions were performed in triplicates. The expression of GAPDH was used for normalization. The $2^{-(\Delta\Delta Cq)}$ method was used to calculate the relative fold changes in mRNA expression

Table 1. List of primer sequences used in this study.

Gene	Forward primer	Reverse primer	Size, bp	Accession #
COL1A1	5′-CAGGAGGCACGCGGAGTGTG-3′	5′-GGCAGGGCTCGGGTTTCCAC-3′	263	NM_000088.4
COL3A1	5′-TCCCGGTCCTGCTGGTTCCC-3′	5′-ATGGCAGCGGCTCCAACACC-3′	390	NM_000090.4
α-SMA	5′-GACAATGGCTCTGGGCTCTGTAA-3′	5′-CTGTGCTTCGTCACCCACGTA-3′	149	NM_001613.4
GAPDH	5′-CAAGGCTGAGAACGGGAAGC-3′	5′-AGGGGGCAGAGATGATGACC-3′	194	NM_001256799.3

5. Immunoblotting analysis

Cells were lysed in sample buffer [62.5 mM Tris-HCl, pH 6.8, 34.7 mM sodium dodecyl sulfate (SDS), 10 % (v/v) glycerol, and 5% (v/v) β-mercaptoethanol], boiled for 5 min, subjected to SDS-polyacrylamide gel electrophoresis, and transferred to an Immobilon membrane (Millipore). After blocking with 5 % skim milk in Tris-HCl-buffered saline containing 0.05 % (v/v) Tween 20 (TBST) for 30 min, the membrane was incubated with primary antibodies against α-SMA, Lats1, PKCδ, pYAP, YAP, and GAPDH at a dilution of 1:1000 or COL1A1, pLats1, pPKCδ, pPKCα/β, pPKCθ, and pPKCζ/λ at a dilution of 1:2000 at 4 °C overnight. The membrane was washed thrice for 5 min with TBST and then incubated with horseradish peroxidase-conjugated secondary antibodies (1:5000) for 1 h. After washing thrice with TBST, protein bands were visualized using an EZ-Western Lumi Pico or Femto kit (Dogen, Seoul, Republic of Korea) according to the manufacturer's instructions and detected using a ChemiDoc XRS+ system (Bio-Rad, Hercules, CA, USA).

6. Immunocytochemical analysis

To detect the localization of the YAP protein, LX-2 cells were grown on glass coverslips and exposed to TPA with or without Gö 6983 for 24 h. Cells were then washed with PBS, fixed with 4 % paraformaldehyde, permeabilized with 0.2 % Triton X-100 for 10 min at 25 °C, and blocked with 3 % FBS in PBS for 30 min and then incubated with

primary antibody specific for YAP (1:100; Santa Cruz) at 4 °C overnight. For fluorescence labeling, cells were incubated with Alexa Fluor 488-conjugated secondary antibody (1:100; Invitrogen, Carlsbad, CA, USA) for 1 h at 25 °C. The unbound secondary antibody was removed by washing and cells were mounted in ProLong™ Gold Antifade Mountant with DAPI. Cells were observed and photographed under a fluorescent microscope (Eclipse TS2R, Nikon, Tokyo, Japan).

7. Cell cycle analysis

Cellular DNA contents were analyzed using the CycleTEST plus DNA reagent kit (BD Biosciences, San Jose, CA, USA) according to the manufacturer's instructions. Briefly, LX-2 cells were trypsinized and centrifuged at 2000 rpm for 5 min. Cells were washed twice with buffer solution provided in the kit and sequentially treated with solutions A, B, and C. DNA contents were analyzed using a flow cytometer (BD FACSAria III, BD Biosciences).

8. Statistical analysis

All experiments were performed thrice. Data are expressed as the mean ± standard deviation. *p* values were determined using a paired two-tailed Student's *t*-test or Mann–Whitney U test. All statistical analyses were performed using the GraphPad Prism 7.0

software (GraphPad Inc., La Jolla, CA). Significance was set at $p \leq 0.05$.

III. Results

1. TPA-induced inhibition of activation of hepatic stellate cells

Although TPA promotes tumor progression and fibrosis, the opposite effects can also occur depending on cell type [44,48]. As a preliminary study, we analyzed the effect of TPA on the proliferation of 2 hepatocellular carcinoma cell lines (HepG2 and Huh-7), hepatic stellate cells (LX-2), and cardiac fibroblasts. When we treated each cell line with 10 nM TPA for 2 days, we found that the proliferation of HepG2 was increased by approximately 36 %, whereas that of Huh-7 cells was not affected. Conversely, treatment of LX-2 cells and cardiac fibroblasts with TPA resulted in a decrease in their proliferation by 27 % and 39 %, respectively (Figure S1). Based on these results, we investigated the mechanisms of TPA on the proliferation of LX-2 cells and expression of α-SMA. We detected that TPA at concentrations above 1 nM decreased the proliferation of LX-2 (Figure 1a), with 10 nM TPA retarding the proliferation rate of LX-2 cells compared with that of the control group in a time-dependent manner (Figure 1b). When we used flow cytometry to analyze the cell cycle at the indicated time-points after TPA treatment, we found that the S and G2/M phases were increased by approximately 3.2 % and 6.3 % at 12 h, whereas the G1 phase was decreased by approximately 10.1 %. Of note, the cell cycle was restored to levels similar to those of the control group at 48 h. Because TPA decreased

the proliferation rate of LX-2 cells (Figure 1a, b) and we rarely observed the apoptotic population in TPA-treated LX-2 cells (Figure 1c), the increase of the G2/M phase at 12 h suggested that TPA was transiently associated with G2/M arrest in LX-2 cells. In addition, we observed that TPA de-creased the expression of *α-SMA*, *COL1A1*, and *COL3A1* mRNA (Figure 1d), and in particular inhibited the expression of α-SMA and COL1A1 in a dose-dependent manner (Figure 1e). These results suggest that TPA induces transient G2/M arrest in LX-2 cells, slowing cell proliferation and effectively inhibiting the expression of α-SMA.

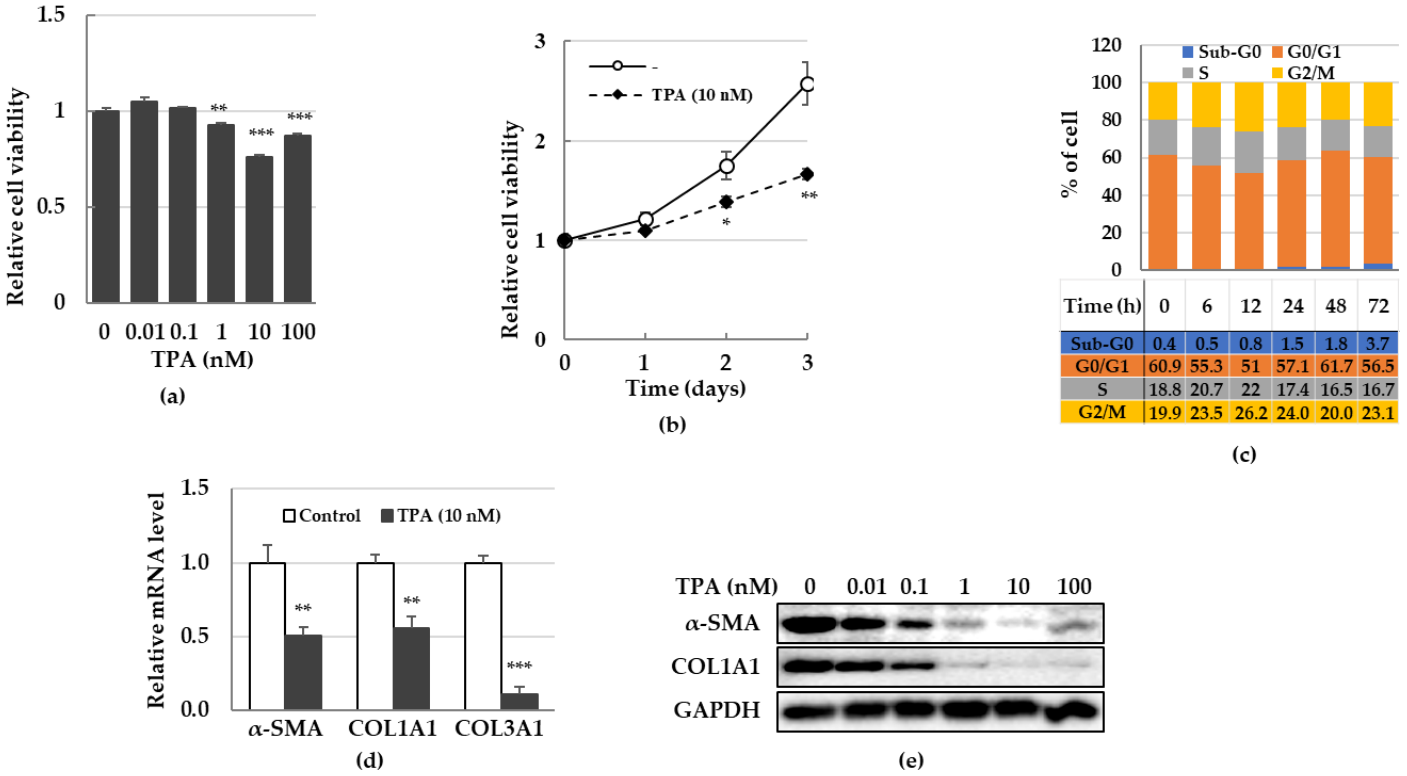

Figure 1. Inhibition of growth and expression of α-SMA in TPA-treated LX-2 cells.

LX-2 cells were treated with up to 100 nM TPA for 2 days and then cell viability and expression of α-SMA were analyzed

using MTT assay and immunoblotting, respectively. On day 2, mRNA expression was assessed by using qPCR, while the cell cycle was examined at the indicated time-points using flow cytometry. (a) LX-2 cell viability according to TPA concentration. Data are presented as the mean ± SD of four independent experiments. $^{**}p \leq 0.01$ and $^{***}p < 0.001$. (b) Proliferation of LX-2 cells treated with 10 nM TPA. Data are presented as the mean ± SD of 4 independent experiments. $^{*}p \leq 0.05$ and $^{**}p \leq 0.01$. (c) Cell cycles of TPA-treated LX-2 cells over time. The percentage of cells was analyzed using 2×10^4 cells in indicated time-points. Data are presented as the mean ± SD of three independent experiments. (d) Expression of *α-SMA*, *COL1A1*, and *COL3A1* mRNA in TPA-treated LX-2 cells. All qPCR reactions were performed in triplicate. Expression of *GAPDH* was used for normalization. The $2^{-(\Delta\Delta Cq)}$ method was used to calculate relative fold changes in mRNA expression. (e) Expression of *α-SMA* and *COL1A1* in TPA-treated LX-2 cells. Data of (d) and (e) are presented as mean ± SD of three independent experiments. $^{*}p \leq 0.05$, $^{**}p \leq 0.01$, and $^{***}p < 0.001$.

2. TPA-induced phosphorylation of PKCδ and YAP in HSCs

TPA acts as a PKC activator [49] and PKCs inhibit the activity of YAP/TAZ [50], which have been associated with the pathophysiology of fibrosis [24,51,52]. Therefore, we investigated which PKC isoforms were activated and whether the phosphorylation or localization of YAP was changed by TPA in LX-2 cells. To detect the phosphorylation of PKCs, we treated LX-2 cells with 10 nM TPA and lysed them at the indicated time-points. We found that the phosphorylation of PKCα/β, PKCθ, and PKCζ/λ was gradually decreased with time compared with that in the control group, whereas the phosphorylation of PKCδ was increased from baseline at 30 min to maximal phosphorylation at approximately 12 h (Figure. 2). Similar to the phosphorylation of PKCδ, we detected that the total levels of PKCδ were gradually increased over 12 h. (Figure 2). These results suggest that TPA regulates the activity of LX-2 cells through the regulation of the activity of PKCδ. As YAP acts downstream of PKCs and the peak phosphorylation of PKCδ was observed at 12 h, we analyzed both the phosphorylation and intracellular localization of YAP on day 1 after TPA treatment. We detected the phosphorylation of LATS and YAP when cells were treated at concentrations above 1 nM TPA (Figure 3a). We observed a significant portion of YAP in the nuclei of cells in the control group, whereas the fluorescence brightness of YAP in the nuclei of TPA-treated LX-2 cells was decreased compared with that in the control group (Figure 3b). These results suggest that greater than 1 nM of TPA increases YAP phosphorylation, which promotes its hydrolysis and further inhibits its nuclear localization, thereby suppressing gene expression, including that of α-SMA.

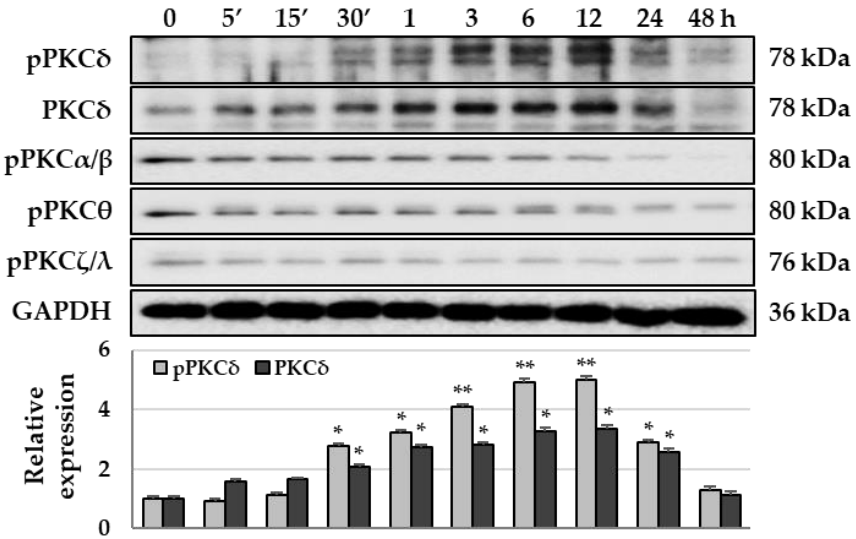

Figure 2. Phosphorylation of PKCs in TPA-treated LX-2 cells.

LX-2 cells were treated with 10 nM TPA for the indicated time, and PKC phosphorylation was detected using the phospho-PKC antibody sampler kit (Cell Signaling Technology). As only the phosphorylation of PKCδ was in-creased in TPA-treated LX-2 cells, we further confirmed the expression of total PKCδ. The intensity of protein expression was quantified using densitometry with Image J and its relative expression was normalized against that of GAPDH. Data are presented as the mean ± SD of three independent experiments. *$p \leq 0.05$ and **$p \leq 0.01$.

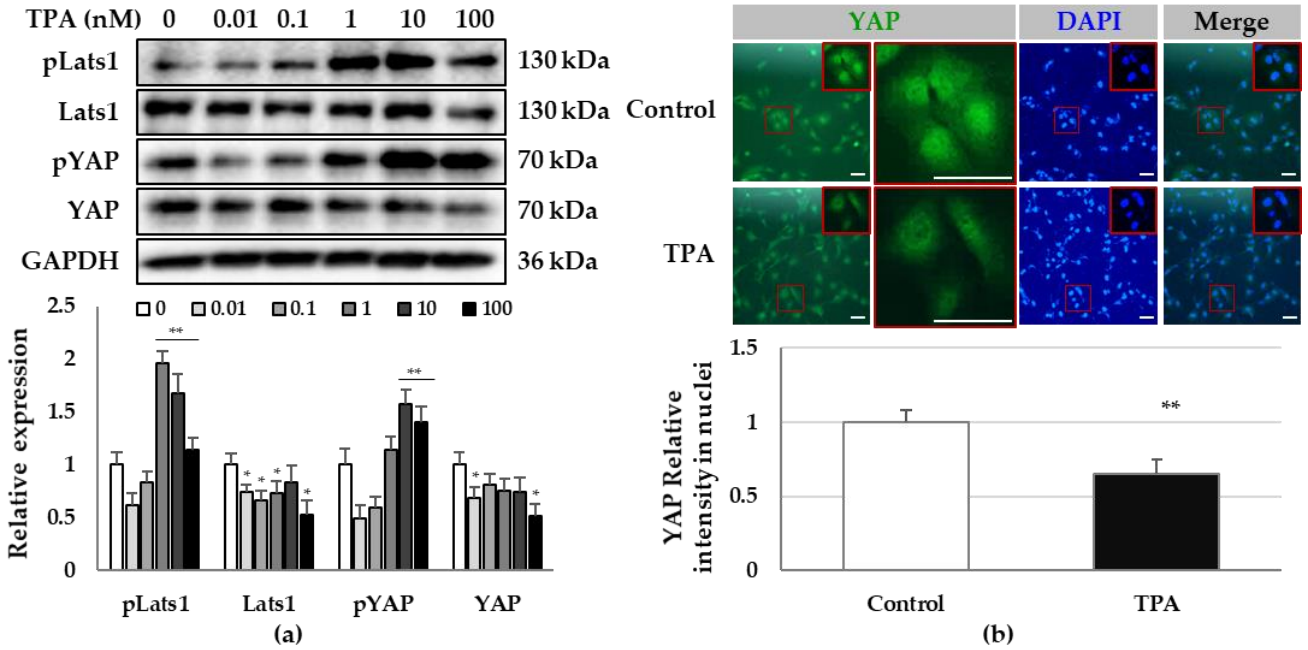

Figure 3. Phosphorylation and cellular distribution of YAP in TPA-treated LX-2 cells.

LX-2 cells were treated with TPA (0.01–100 nM) for 24 h. The phosphorylation and cellular distribution of YAP were detected using immunoblotting and immunocytochemistry, respectively, in LX-2 cells treated with 10 nM TPA for 24 h. (a) Phosphorylation of LATS1 and YAP in LX-2 cells. The intensity of protein expression was quantified using densitometry with Image J and its relative ex-pression was normalized against that of GAPDH. Data are presented as the mean ± SD of

three independent experiments. *$p \leq 0.05$ and **$p \leq 0.01$. (b) Cellular distribution of YAP in TPA-treated LX-2 cells. The nuclear fluorescence intensity of YAP was quantified using densitometry with Image J. Nuclear fluorescence intensity was analyzed from three random fields, with over 30 cells counted per field. Data are presented as the mean ± SD of three independent experiments. **$p \leq 0.01$. Scale bar, 20 μm.

3. Roles of PKCδ and YAP in HSC activation.

Next, we investigated whether the pan-PKC inhibitor, Gö 6983, could restore the TPA-induced inhibition of proliferation and decrease in the expression of α-SMA in LX-2 cells. To detect whether Gö 6983 inhibited the phosphorylation of PKCδ, we exposed LX-2 cells to 1 μM Gö 6983 20 min prior to TPA treatment. We found that the TPA-induced phosphorylation of PKCδ was abolished by Gö 6983 at 12 h (Figure 4c). In addition, the TPA-induced reduction in cell proliferation was recovered to control levels by Gö 6983 (Figure 4a), while also no G2/M arrest was observed in LX-2 cells treated with TPA + Gö 6983 at 12 h (Figure 4b). We further noticed that the decrease in the expression of *α-SMA*, *COL1A1*, and *COL3A1* mRNA as well as the levels of α-SMA and COL1A1 proteins were also restored by Gö 6983 (Figure 4d, e). These results suggest that the activation of PKCδ plays an important role in the regulation of the activation of LX-2 cells which is represented by an increase in proliferation potential and expression of α-SMA.

Furthermore, it was observed that Gö 6983 decreased the TPA-induced phosphorylation of YAP (Figure 5a) with most YAP being located in the nuclei of LX-2 cells similar to the control group (Figure 5b). These results suggest that YAP phosphorylation inhibits the translocation of YAP into the nucleus. Therefore, TPA induces phosphorylation of PKCδ and YAP to inhibit the translocation of YAP into the nucleus, leading to growth suppression and a decrease in the expression of α-SMA in LX-2 cells. Therefore, PKCδ and YAP can be utilized as targets to regulate the activity of hepatic stellate cells for the treatment of fibrosis.

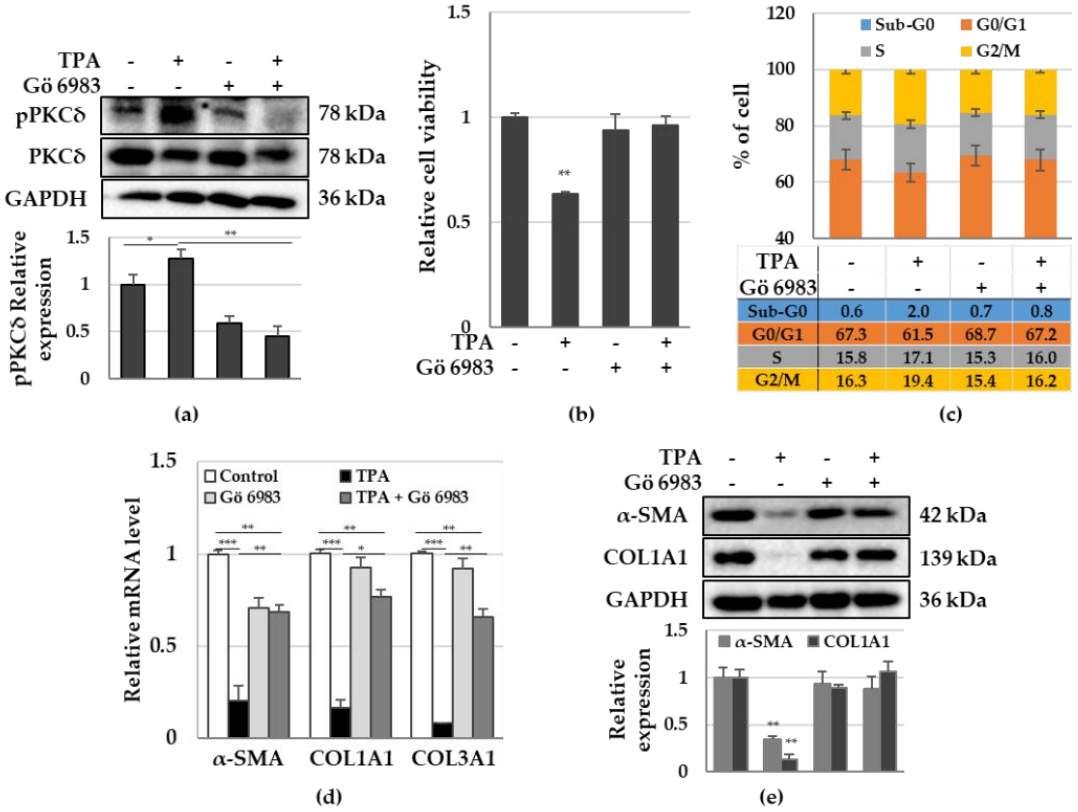

Figure 4. Effects of the pan-PKC inhibitor Gö 6983 on the proliferation and fibrosis of TPA-treated LX-2 cells.

LX-2 cells were treated with TPA (10 nM) or Gö 6983 (1 μM) or both, and then cell viability, cell cycle, and expression of

α-SMA were analyzed. (a) PKCδ phosphorylation in LX-2 cells treated with TPA or Gö 6983 or both for 12 h. The intensity of pPKCδ was quantified using densitometry with Image J and its relative expression was normalized against that of GAPDH. Data are presented as the mean ± SD of 3 independent experiments. *$p \leq 0.05$ and **$p \leq 0.01$. (b) LX-2 cell viability after treatment with TPA or Gö 6983 or both for 48 h. Data are presented as the mean ± SD of four independent experiments. **$p \leq 0.01$. (c) Cell cycles of LX-2 cells treated with TPA or Gö 6983 or both. The percentage of cells was analyzed using 2×10^4 cells treated with TPA or Gö 6983 or both for 12 h. Data are presented as the mean ± SD of three independent experiments. (d) Expression of *α-SMA*, *COL1A1*, and *COL3A1* mRNA in LX-2 cells treated with TPA or Gö 6983 or both for 48 h. All qPCR reactions were performed in triplicate. Expression of *GAPDH* was used for normalization. The $2^{-(\Delta\Delta Cq)}$ method was used to calculate relative fold changes in mRNA expression. Data are presented as the mean ± SD of three independent experiments. *$p \leq 0.05$, **$p \leq 0.01$, and ***$p < 0.001$. (e) Expression of α-SMA and COL1A1 in LX-2 cells treated with TPA or Gö 6983 or both for 48 h. The intensity of protein expression was quantified using densitometry with Image J and its relative expression was normalized against that of GAPDH. Data are presented as the mean ± SD of three independent experiments. **$p \leq 0.01$.

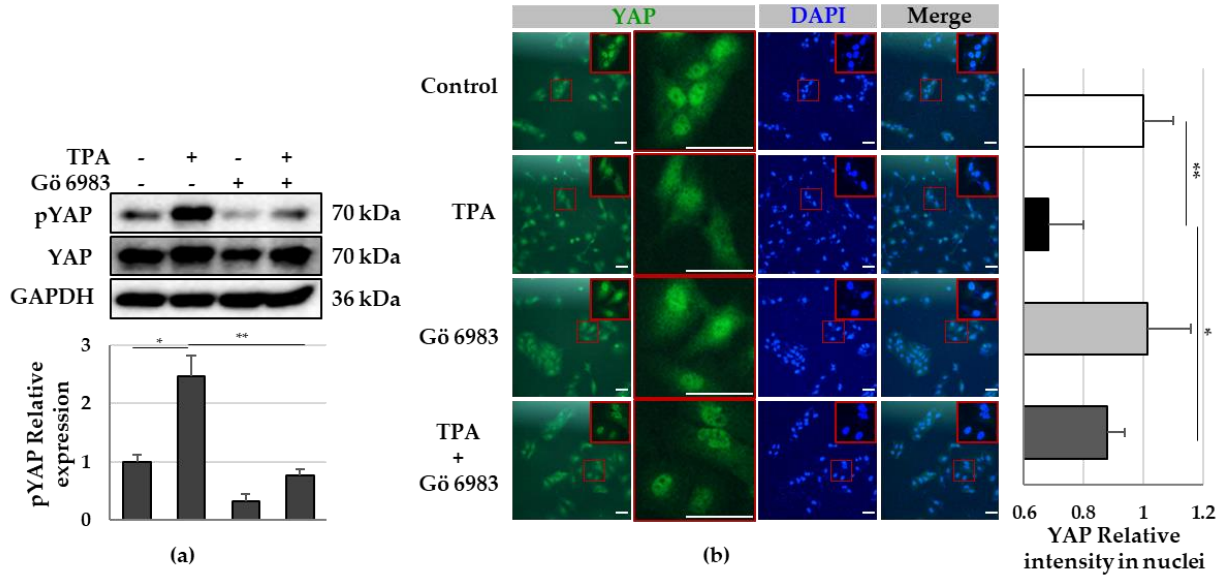

Figure 5. Phosphorylation and cellular distribution of YAP in LX-2 cells treated with TPA or Gö 6983 or both.

LX-2 cells were treated with TPA (10 nM) or Gö 6983 (1 μM) or both for 24 h. The phosphorylation and cellular distribution of YAP was detected using immunoblotting and immunocytochemistry, respectively. (a) YAP phosphorylation in LX-2 cells.

The intensity of pYAP was quantified using densitometry with Image J and its relative expression was normalized against that of GAPDH. Data are presented as the mean ± SD of three independent experiments. *$p \leq 0.05$ and **$p \leq 0.01$. (b) Cellular distribution of YAP in LX-2 cells treated with TPA or Gö 6983 or both. The nuclear fluorescence intensity of YAP was quantified using densitometry with Image J. Nuclear fluorescence intensity was analyzed from three random fields, with over 30 cells counted per field. Data are presented as the mean ± SD of three independent experiments. *$p \leq 0.05$ and **$p \leq 0.01$. Scale bar, 20 μm.

IV. Discussion

In this study, we observed that TPA induced transient G2/M arrest, growth inhibition, and a decrease in the expression of α-SMA in LX-2 cells. In addition, TPA increased the phosphorylation of PKCδ and YAP, whereas decreased the nuclear translocation of YAP. However, administration of the pan-PKC inhibitor Gö 6983 ameliorated these TPA-induced responses in LX-2 cells. Our results suggest that the regulation of the activity of PKCδ and YAP can be utilized as a target strategy for controlling the proliferation and fibrosis of hepatic stellate cells.

The majority of the reports suggest that PKC promotes fibrosis. Inhibition of PKCα, -β, and -λ or θ is involved in antifibrotic or fibrotic effects, respectively. Here, the phosphorylation of PKCα/β, PKCθ, and PKCζ/λ was gradually decreased with time compared to the control group. Since the antifibrotic effect induced by TPA in LX-2 cells may be regulated by dephosphorylation of PKCα/β and PKCζ/λ, further study is needed to evaluate whether a specific activator of the PKC isoform can modulate LX-2 fibrosis.

PKCδ affects not only cell growth and proliferation, but also inflammatory responses and the activation of inflammatory cells [53-57]. In addition, the PKCδ expression has been reported to be increased in fibrotic tissues, with PKCδ regulating the expression of collagen and α-SMA genes [58-61]. However, in this study, the expression of α-SMA and COL1A1 was significantly suppressed in LX-2 cells, despite the TPA-induced increase in the

expression and phosphorylation of PKCδ. The pan-PKC inhibitor, Gö 6983 decreased the phosphorylation of PKCδ, resulting in the recovery of the growth rate and levels of expression of α-SMA and COL1A1. Consistent with our results, Karhu *et al*. reported that TPA reduced cell viability and the expression of α-SMA in cardiac fibroblasts via c- and nPKCs [48], despite not showing whether TPA induced the phosphorylation of PKCs. Therefore, PKCs, including PKCδ, are considered important molecules in regulating fibrosis or antifibrosis in different cell types. Recently, the Hippo pathway was shown to contribute to the pathogenesis of fibrosis, in which hyperactive YAP and TAZ accumulates in both the epithelial and stromal compartments of fibrotic tissues, including the lung, kidney, liver, heart, skin, and tumor. YAP and TAZ are the main downstream effectors of the mammalian Hippo pathway, which exerts a crucial role in controlling tissue and organ development, fibrosis, and tumorigenesis. Gong *et al*. [62] suggested that TPA-activated PKCs might be linked to the activation of YAP/TAZ. Briefly, they found that TPA activated PKCs, inducing the rapid and potent dephosphorylation of YAP (Ser-127) in HEK293A, HeLa, and U251 cells [62]. Conversely, TPA induced the phosphorylation of YAP/TAZ in MEF, A549, and Swiss3T3 cells. They explained that cPKCs promoted the dephosphorylation and activation of YAP, but overexpression of nPKC (δ, θ, or ε) blocked the TPA-induced dephosphorylation of YAP, with nPKC (η) promoting the phosphorylation of YAP in HEK293A cells. To confirm the phosphorylation or dephosphorylation status of YAP, HEK293A, HeLa, and U251 cells or MEF, A549, and Swiss3T3 cells were treated with TPA under serum-free or -complete conditions, respectively. In addition, although

serum induces the dephosphorylation of YAP in HEK293A cells, Gong *et al*. showed that the ectopic expression of PKCε induced the phosphorylation of YAP even in the presence of serum. In particular, the ectopic expression of PKCδ, PKCθ, and PKCη induced a mild-to-moderate increase in the phosphorylation of YAP [62]. Here, we used media supplemented with serum to treat LX-2 cells with TPA and then observed that the level of ex-pression and phosphorylation of PKCδ was gradually increased. Therefore, our results suggest that in LX-2 cells in the presence of serum, TPA induces the expression and phosphorylation of PKCδ and the phosphorylation and cytosolic localization of YAP, leading to the suppression of the expression of α-SMA. Thus, we hypothesized that the regulation of YAP phosphorylation in different cells depends on the level of expression and phosphorylation of PKCs and the presence of serum. Indeed, at 24 h after seeding LX-2 cells under serum conditions, the expression of α-SMA (Figure S2a) and nuclear localization of YAP (Figure S2b) was rarely observed, whereas both the nuclear translocation of YAP and expression of α-SMA at day 2 was significantly increased compared with those at day 0 control cells (Figure S2). These results suggest that the activity of LX-2 cells can be regulated depending on the serum status; more precisely, in the presence of serum, TPA phosphorylates PKCδ, then phosphorylates YAP, and inhibits the nuclear translocation of YAP, resulting in the suppression of the activation of HSCs.

To further demonstrate that PKCδ and YAP are involved in the suppression of the activation of HSCs, additional studies are needed to demonstrate the regulation of PKCs and YAP functions through the overexpression or down-regulation of their expression.

Supplementary Materials: The following supporting information can be downloaded at:, https://www.mdpi.com/article/10.3390/cells12010091/s1, Figure S1: Effect of TPA on the proliferation of several cells; Figure S2: expression of α-SMA and nuclear translocation of YAP in LX-2 cells.

References

1. Reynaert, H.; Thompson, M.G.; Thomas, T.; Geerts, A. Hepatic stellate cells: role in microcirculation and pathophysiology of portal hypertension. *Gut* **2002**, *50*, 571-581, doi:10.1136/gut.50.4.571.

2. Geerts, A. History, heterogeneity, developmental biology, and functions of quiescent hepatic stellate cells. *Semin Liver Dis* **2001**, *21*, 311-335, doi:10.1055/s-2001-17550.

3. Friedman, S.L. Hepatic stellate cells: protean, multifunctional, and enigmatic cells of the liver. *Physiol Rev* **2008**, *88*, 125-172, doi:10.1152/physrev.00013.2007.

4. Trivedi, P.; Wang, S.; Friedman, S.L. The Power of Plasticity-Metabolic Regulation of Hepatic Stellate Cells. *Cell Metab* **2021**, *33*, 242-257, doi:10.1016/j.cmet.2020.10.026.

5. Baghaei, K.; Mazhari, S.; Tokhanbigli, S.; Parsamanesh, G.; Alavifard, H.; Schaafsma, D.; Ghavami, S. Therapeutic potential of targeting regulatory mechanisms of hepatic stellate cell activation in liver fibrosis. *Drug Discov Today* **2022**, *27*, 1044-1061, doi:10.1016/j.drudis.2021.12.012.

6. Fabregat, I.; Moreno-Caceres, J.; Sanchez, A.; Dooley, S.; Dewidar, B.; Giannelli, G.; Ten Dijke, P.; Consortium, I.-L. TGF-beta signalling and liver disease. *FEBS J* **2016**, *283*, 2219-2232, doi:10.1111/febs.13665.

7. Bartneck, M.; Koppe, C.; Fech, V.; Warzecha, K.T.; Kohlhepp, M.; Huss, S.;

Weiskirchen, R.; Trautwein, C.; Luedde, T.; Tacke, F. Roles of CCR2 and CCR5 for Hepatic Macrophage Polarization in Mice With Liver Parenchymal Cell-Specific NEMO Deletion. *Cell Mol Gastroenterol Hepatol* **2021**, *11*, 327-347, doi:10.1016/j.jcmgh.2020.08.012.

8. Hellerbrand, C.; Jobin, C.; Licato, L.L.; Sartor, R.B.; Brenner, D.A. Cytokines induce NF-kappaB in activated but not in quiescent rat hepatic stellate cells. *Am J Physiol* **1998**, *275*, G269-278, doi:10.1152/ajpgi.1998.275.2.G269.

9. Lee, M.; Lee, Y.; Song, J.; Lee, J.; Chang, S.Y. Tissue-specific Role of CX3CR1 Expressing Immune Cells and Their Relationships with Human Disease. *Immune Netw* **2018**, *18*, e5, doi:10.4110/in.2018.18.e5.

10. Sahin, H.; Borkham-Kamphorst, E.; Kuppe, C.; Zaldivar, M.M.; Grouls, C.; Al-samman, M.; Nellen, A.; Schmitz, P.; Heinrichs, D.; Berres, M.L., et al. Chemokine Cxcl9 attenuates liver fibrosis-associated angiogenesis in mice. *Hepatology* **2012**, *55*, 1610-1619, doi:10.1002/hep.25545.

11. Ballardini, G.; Degli Esposti, S.; Bianchi, F.B.; de Giorgi, L.B.; Faccani, A.; Biolchini, L.; Busachi, C.A.; Pisi, E. Correlation between Ito cells and fibrogenesis in an experimental model of hepatic fibrosis. A sequential stereological study. *Liver* **1983**, *3*, 58-63, doi:10.1111/j.1600-0676.1983.tb00850.x.

12. Reeves, H.L.; Burt, A.D.; Wood, S.; Day, C.P. Hepatic stellate cell activation occurs

in the absence of hepatitis in alcoholic liver disease and correlates with the severity of steatosis. *J Hepatol* **1996**, *25*, 677-683, doi:10.1016/s0168-8278(96)80238-8.

13. Mochly-Rosen, D.; Das, K.; Grimes, K.V. Protein kinase C, an elusive therapeutic target? *Nat Rev Drug Discov* **2012**, *11*, 937-957, doi:10.1038/nrd3871.

14. Umar, S.; Sellin, J.H.; Morris, A.P. Increased nuclear translocation of catalytically active PKC-zeta during mouse colonocyte hyperproliferation. *Am J Physiol Gastrointest Liver Physiol* **2000**, *279*, G223-237, doi:10.1152/ajpgi.2000.279.1.G223.

15. Musashi, M.; Ota, S.; Shiroshita, N. The role of protein kinase C isoforms in cell proliferation and apoptosis. *Int J Hematol* **2000**, *72*, 12-19.

16. Murphy, T.L.; Sakamoto, T.; Hinton, D.R.; Spee, C.; Gundimeda, U.; Soriano, D.; Gopalakrishna, R.; Ryan, S.J. Migration of retinal pigment epithelium cells in vitro is regulated by protein kinase C. *Exp Eye Res* **1995**, *60*, 683-695, doi:10.1016/s0014-4835(05)80010-7.

17. Steinberg, S.F. Structural basis of protein kinase C isoform function. *Physiol Rev* **2008**, *88*, 1341-1378, doi:10.1152/physrev.00034.2007.

18. Palaniyandi, S.S.; Sun, L.; Ferreira, J.C.; Mochly-Rosen, D. Protein kinase C in heart failure: a therapeutic target? *Cardiovasc Res* **2009**, *82*, 229-239, doi:10.1093/cvr/cvp001.

19. O'Brian, C.A.; Liskamp, R.M.; Solomon, D.H.; Weinstein, I.B. Inhibition of protein

kinase C by tamoxifen. *Cancer Res* **1985**, *45*, 2462-2465.

20. Schwartz, G.K.; Jiang, J.; Kelsen, D.; Albino, A.P. Protein kinase C: a novel target for inhibiting gastric cancer cell invasion. *J Natl Cancer Inst* **1993**, *85*, 402-407, doi:10.1093/jnci/85.5.402.

21. Liu, Q.; Chen, X.; Macdonnell, S.M.; Kranias, E.G.; Lorenz, J.N.; Leitges, M.; Houser, S.R.; Molkentin, J.D. Protein kinase C{alpha}, but not PKC{beta} or PKC{gamma}, regulates contractility and heart failure susceptibility: implications for ruboxistaurin as a novel therapeutic approach. *Circ Res* **2009**, *105*, 194-200, doi:10.1161/CIRCRESAHA.109.195313.

22. Ferreira, J.C.; Koyanagi, T.; Palaniyandi, S.S.; Fajardo, G.; Churchill, E.N.; Budas, G.; Disatnik, M.H.; Bernstein, D.; Brum, P.C.; Mochly-Rosen, D. Pharmacological inhibition of betaIIPKC is cardioprotective in late-stage hypertrophy. *J Mol Cell Cardiol* **2011**, *51*, 980-987, doi:10.1016/j.yjmcc.2011.08.025.

23. Inagaki, K.; Koyanagi, T.; Berry, N.C.; Sun, L.; Mochly-Rosen, D. Pharmacological inhibition of epsilon-protein kinase C attenuates cardiac fibrosis and dysfunction in hypertension-induced heart failure. *Hypertension* **2008**, *51*, 1565-1569, doi:10.1161/HYPERTENSIONAHA.107.109637.

24. Piersma, B.; Bank, R.A.; Boersema, M. Signaling in Fibrosis: TGF-beta, WNT, and YAP/TAZ Converge. *Front Med (Lausanne)* **2015**, *2*, 59,

doi:10.3389/fmed.2015.00059.

25. Kisseleva, T.; Uchinami, H.; Feirt, N.; Quintana-Bustamante, O.; Segovia, J.C.; Schwabe, R.F.; Brenner, D.A. Bone marrow-derived fibrocytes participate in pathogenesis of liver fibrosis. *J Hepatol* **2006**, *45*, 429-438, doi:10.1016/j.jhep.2006.04.014.

26. Shi, Y.; Massague, J. Mechanisms of TGF-beta signaling from cell membrane to the nucleus. *Cell* **2003**, *113*, 685-700, doi:10.1016/s0092-8674(03)00432-x.

27. Bujak, M.; Ren, G.; Kweon, H.J.; Dobaczewski, M.; Reddy, A.; Taffet, G.; Wang, X.F.; Frangogiannis, N.G. Essential role of Smad3 in infarct healing and in the pathogenesis of cardiac remodeling. *Circulation* **2007**, *116*, 2127-2138, doi:10.1161/CIRCULATIONAHA.107.704197.

28. Wang, B.; Omar, A.; Angelovska, T.; Drobic, V.; Rattan, S.G.; Jones, S.C.; Dixon, I.M. Regulation of collagen synthesis by inhibitory Smad7 in cardiac myofibroblasts. *Am J Physiol Heart Circ Physiol* **2007**, *293*, H1282-1290, doi:10.1152/ajpheart.00910.2006.

29. Springer, J.; Scholz, F.R.; Peiser, C.; Groneberg, D.A.; Fischer, A. SMAD-signaling in chronic obstructive pulmonary disease: transcriptional down-regulation of inhibitory SMAD 6 and 7 by cigarette smoke. *Biol Chem* **2004**, *385*, 649-653, doi:10.1515/BC.2004.080.

30. Pulichino, A.M.; Wang, I.M.; Caron, A.; Mortimer, J.; Auger, A.; Boie, Y.; Elias, J.A.; Kartono, A.; Xu, L.; Menetski, J., et al. Identification of transforming growth factor beta1-driven genetic programs of acute lung fibrosis. *Am J Respir Cell Mol Biol* **2008**, *39*, 324-336, doi:10.1165/rcmb.2007-0186OC.

31. Liu, C.; Gaca, M.D.; Swenson, E.S.; Vellucci, V.F.; Reiss, M.; Wells, R.G. Smads 2 and 3 are differentially activated by transforming growth factor-beta (TGF-beta) in quiescent and activated hepatic stellate cells. Constitutive nuclear localization of Smads in activated cells is TGF-beta-independent. *J Biol Chem* **2003**, *278*, 11721-11728, doi:10.1074/jbc.M207728200.

32. Kaimori, A.; Potter, J.; Kaimori, J.Y.; Wang, C.; Mezey, E.; Koteish, A. Transforming growth factor-beta1 induces an epithelial-to-mesenchymal transition state in mouse hepatocytes in vitro. *J Biol Chem* **2007**, *282*, 22089-22101, doi:10.1074/jbc.M700998200.

33. Poncelet, A.C.; Schnaper, H.W.; Tan, R.; Liu, Y.; Runyan, C.E. Cell phenotype-specific down-regulation of Smad3 involves decreased gene activation as well as protein degradation. *J Biol Chem* **2007**, *282*, 15534-15540, doi:10.1074/jbc.M701991200.

34. Meng, X.M.; Huang, X.R.; Chung, A.C.; Qin, W.; Shao, X.; Igarashi, P.; Ju, W.; Bottinger, E.P.; Lan, H.Y. Smad2 protects against TGF-beta/Smad3-mediated renal fibrosis. *J Am Soc Nephrol* **2010**, *21*, 1477-1487, doi:10.1681/ASN.2009121244.

35. Ashcroft, G.S.; Yang, X.; Glick, A.B.; Weinstein, M.; Letterio, J.L.; Mizel, D.E.; Anzano, M.; Greenwell-Wild, T.; Wahl, S.M.; Deng, C., et al. Mice lacking Smad3 show accelerated wound healing and an impaired local inflammatory response. *Nat Cell Biol* **1999**, *1*, 260-266, doi:10.1038/12971.

36. Wei, J.; Fang, F.; Lam, A.P.; Sargent, J.L.; Hamburg, E.; Hinchcliff, M.E.; Gottardi, C.J.; Atit, R.; Whitfield, M.L.; Varga, J. Wnt/beta-catenin signaling is hyperactivated in systemic sclerosis and induces Smad-dependent fibrotic responses in mesenchymal cells. *Arthritis Rheum* **2012**, *64*, 2734-2745, doi:10.1002/art.34424.

37. Kapoor, M.; Liu, S.; Shi-wen, X.; Huh, K.; McCann, M.; Denton, C.P.; Woodgett, J.R.; Abraham, D.J.; Leask, A. GSK-3beta in mouse fibroblasts controls wound healing and fibrosis through an endothelin-1-dependent mechanism. *J Clin Invest* **2008**, *118*, 3279-3290, doi:10.1172/JCI35381.

38. Hamburg, E.J.; Atit, R.P. Sustained beta-catenin activity in dermal fibroblasts is sufficient for skin fibrosis. *J Invest Dermatol* **2012**, *132*, 2469-2472, doi:10.1038/jid.2012.155.

39. Fukushima, K.; Takahashi, K.; Fukushima, N.; Honoki, K.; Tsujiuchi, T. Different effects of GPR120 and GPR40 on cellular functions stimulated by 12-O-tetradecanoylphorbol-13-acetate in melanoma cells. *Biochem Biophys Res Commun* **2016**, *475*, 25-30, doi:10.1016/j.bbrc.2016.05.023.

40. Lii, C.K.; Chang, J.W.; Chen, J.J.; Chen, H.W.; Liu, K.L.; Yeh, S.L.; Wang, T.S.; Liu, S.H.; Tsai, C.H.; Li, C.C. Docosahexaenoic acid inhibits 12-O-tetradecanoylphorbol-13- acetate-induced fascin-1-dependent breast cancer cell migration by suppressing the PKCdelta- and Wnt-1/beta-catenin-mediated pathways. *Oncotarget* **2016**, *7*, 25162-25179, doi:10.18632/oncotarget.7301.

41. Slaga, T.J.; Scribner, J.D.; Viaje, A. Epidermal cell proliferation and promoting ability of phorbol esters. *J Natl Cancer Inst* **1976**, *57*, 1145-1149, doi:10.1093/jnci/57.5.1145.

42. Alfredsson, C.F.; Rendel, F.; Liang, Q.L.; Sundstrom, B.E.; Nanberg, E. Altered sensitivity to ellagic acid in neuroblastoma cells undergoing differentiation with 12-O-tetradecanoylphorbol-13-acetate and all-trans retinoic acid. *Biomed Pharmacother* **2015**, *76*, 39-45, doi:10.1016/j.biopha.2015.10.008.

43. Strair, R.K.; Schaar, D.; Goodell, L.; Aisner, J.; Chin, K.V.; Eid, J.; Senzon, R.; Cui, X.X.; Han, Z.T.; Knox, B., et al. Administration of a phorbol ester to patients with hematological malignancies: preliminary results from a phase I clinical trial of 12-O-tetradecanoylphorbol-13-acetate. *Clin Cancer Res* **2002**, *8*, 2512-2518.

44. Zhu, G.; Chen, Y.; Zhang, X.; Wu, Q.; Zhao, Y.; Chen, Y.; Sun, F.; Qiao, Y.; Wang, J. 12-O-Tetradecanoylphorbol-13-acetate (TPA) is anti-tumorigenic in liver cancer cells via inhibiting YAP through AMOT. *Sci Rep* **2017**, *7*, 44940, doi:10.1038/srep44940.

45. Mulsow, J.J.; Watson, R.W.; Fitzpatrick, J.M.; O'Connell, P.R. Transforming growth

factor-beta promotes pro-fibrotic behavior by serosal fibroblasts via PKC and ERK1/2 mitogen activated protein kinase cell signaling. *Ann Surg* **2005**, *242*, 880-887, discussion 887-889, doi:10.1097/01.sla.0000189606.58343.cd.

46. Slattery, C.; Ryan, M.P.; McMorrow, T. Protein kinase C beta overexpression induces fibrotic effects in human proximal tubular epithelial cells. *Int J Biochem Cell Biol* **2008**, *40*, 2218-2229, doi:10.1016/j.biocel.2008.03.005.

47. Song, X.; Qian, X.; Shen, M.; Jiang, R.; Wagner, M.B.; Ding, G.; Chen, G.; Shen, B. Protein kinase C promotes cardiac fibrosis and heart failure by modulating galectin-3 expression. *Biochim Biophys Acta* **2015**, *1853*, 513-521, doi:10.1016/j.bbamcr.2014.12.001.

48. Karhu, S.T.; Ruskoaho, H.; Talman, V. Distinct Regulation of Cardiac Fibroblast Proliferation and Transdifferentiation by Classical and Novel Protein Kinase C Isoforms: Possible Implications for New Antifibrotic Therapies. *Mol Pharmacol* **2021**, *99*, 104-113, doi:10.1124/molpharm.120.000094.

49. Tahara, E.; Kadara, H.; Lacroix, L.; Lotan, D.; Lotan, R. Activation of protein kinase C by phorbol 12-myristate 13-acetate suppresses the growth of lung cancer cells through KLF6 induction. *Cancer Biol Ther* **2009**, *8*, 801-807, doi:10.4161/cbt.8.9.8186.

50. Gomes, G.; Bagri, K.M.; de Andrade Rosa, I.; Jurberg, A.D.; Mermelstein, C.; Costa,

M.L. Activation of YAP regulates muscle fiber size in a PKC-dependent mechanism during chick in vitro myogenesis. *J Muscle Res Cell Motil* **2022**, *43*, 73-86, doi:10.1007/s10974-021-09608-8.

51. Mitani, A.; Nagase, T.; Fukuchi, K.; Aburatani, H.; Makita, R.; Kurihara, H. Transcriptional coactivator with PDZ-binding motif is essential for normal alveolarization in mice. *Am J Respir Crit Care Med* **2009**, *180*, 326-338, doi:10.1164/rccm.200812-1827OC.

52. Xin, M.; Kim, Y.; Sutherland, L.B.; Murakami, M.; Qi, X.; McAnally, J.; Porrello, E.R.; Mahmoud, A.I.; Tan, W.; Shelton, J.M., et al. Hippo pathway effector Yap promotes cardiac regeneration. *Proc Natl Acad Sci U S A* **2013**, *110*, 13839-13844, doi:10.1073/pnas.1313192110.

53. Jackson, D.N.; Foster, D.A. The enigmatic protein kinase Cdelta: complex roles in cell proliferation and survival. *FASEB J* **2004**, *18*, 627-636, doi:10.1096/fj.03-0979rev.

54. Steinberg, S.F. Distinctive activation mechanisms and functions for protein kinase Cdelta. *Biochem J* **2004**, *384*, 449-459, doi:10.1042/BJ20040704.

55. Vallee, S.; Laforest, S.; Fouchier, F.; Montero, M.P.; Penel, C.; Champion, S. Cytokine-induced upregulation of NF-kappaB, IL-8, and ICAM-1 is dependent on colonic cell polarity: implication for PKCdelta. *Exp Cell Res* **2004**, *297*, 165-185, doi:10.1016/j.yexcr.2004.03.007.

56. Wang, Q.; Wang, X.; Evers, B.M. Induction of cIAP-2 in human colon cancer cells through PKC delta/NF-kappa B. *J Biol Chem* **2003**, *278*, 51091-51099, doi:10.1074/jbc.M306541200.

57. Page, K.; Li, J.; Zhou, L.; Iasvovskaia, S.; Corbit, K.C.; Soh, J.W.; Weinstein, I.B.; Brasier, A.R.; Lin, A.; Hershenson, M.B. Regulation of airway epithelial cell NF-kappa B-dependent gene expression by protein kinase C delta. *J Immunol* **2003**, *170*, 5681-5689, doi:10.4049/jimmunol.170.11.5681.

58. Jimenez, S.A.; Gaidarova, S.; Saitta, B.; Sandorfi, N.; Herrich, D.J.; Rosenbloom, J.C.; Kucich, U.; Abrams, W.R.; Rosenbloom, J. Role of protein kinase C-delta in the regulation of collagen gene expression in scleroderma fibroblasts. *J Clin Invest* **2001**, *108*, 1395-1403, doi:10.1172/JCI12347.

59. Gore-Hyer, E.; Pannu, J.; Smith, E.A.; Grotendorst, G.; Trojanowska, M. Selective stimulation of collagen synthesis in the presence of costimulatory insulin signaling by connective tissue growth factor in scleroderma fibroblasts. *Arthritis Rheum* **2003**, *48*, 798-806, doi:10.1002/art.10953.

60. Runyan, C.E.; Schnaper, H.W.; Poncelet, A.C. Smad3 and PKCdelta mediate TGF-beta1-induced collagen I expression in human mesangial cells. *Am J Physiol Renal Physiol* **2003**, *285*, F413-422, doi:10.1152/ajprenal.00082.2003.

61. Lee, S.J.; Kang, J.H.; Choi, S.Y.; Suk, K.T.; Kim, D.J.; Kwon, O.S. PKCdelta as a

regulator for TGFbeta1-induced alpha-SMA production in a murine nonalcoholic steatohepatitis model. *PLoS One* **2013**, *8*, e55979, doi:10.1371/journal.pone.0055979.

62. Gong, R.; Hong, A.W.; Plouffe, S.W.; Zhao, B.; Liu, G.; Yu, F.X.; Xu, Y.; Guan, K.L. Opposing roles of conventional and novel PKC isoforms in Hippo-YAP pathway regulation. *Cell Res* **2015**, *25*, 985-988, doi:10.1038/cr.2015.88.

국문 초록

12-O-Tetradecanoylphorbol-13-acetate (TPA)에 의한 간성상세포의 섬유화 활성억제 기전 규명

연세대학교 대학원

의학과

김 창 완

PKC(Protein kinase C)가 세포 증식, 분화, 이동, 조직 재형성, 유전자 발현, 세포 사멸 등 다양한 생물학적 활성을 조절할 수 있지만, 근섬유아세포에서 PKC 의 항섬유화 효과는 완전히 이해되지 않았다. PKC 활성화제인 12-O-tetradecanoylphorbol-13-acetate(TPA)가 간 성상 세포(HSC)의 활성화를 감소시켰는지 여부와 Hippo 경로 전사조절 도움인자 YAP 가 이 활동의 조절에 관여할 수 있는지 여부를 조사했으며 HSC 세포주, LX-2 에서 TPA 가 증식 및 α-평활근 액틴(SMA) 발현에 미치는 영향을 분석했다. Hippo 경로 분자 YAP 및 Lats1 의 인산화 및 YAP 의 핵 전위도 분석하였다. 또한, pan-PKC 억제제인

Go 6983 이 TPA 에 의해 억제된 HSC 활성을 회복시키는지 여부를 조사하였다. LX-2 세포의 성장 속도는 감소되었고 α-SMA 및 콜라겐 유형 I 알파 1(COL1A1) 발현은 TPA 에 의해 억제되었다. 또한, TPA 는 대조군에 비해 PKCδ, Lats1 및 YAP 를 인산화시키고 YAP 가 핵으로의 전위를 억제하였다. TPA 에 의해 발생하는 성장 억제, α-SMA 발현 억제, YAP 의 인산화 및 핵으로의 YAP 전위를 포함한 이러한 현상은 대부분 Go 6983 에 의해 억제되었다. 결론적으로 TPA 는 PKCδ 활성화 및 YAP 활성 억제를 통해 HSC 의 성장 및 α-SMA 발현을 감소시켰다. 본 연구 결과에서 PKCδ가 HSC 에서 Hippo 경로를 억제함으로써 항섬유화 효과가 있음을 시사했으며, 이에 따라 PKCδ와 YAP 는 인산화를 증가시키는 전략을 사용하여 섬유성 질환의 치료 표적으로 사용할 수 있을 것으로 사료된다.

핵심 되는 말: 12-O-tetradecanoylphorbol-13-acetate (TPA), 간성상세포, protein kinase C (PKC)-δ, Yes-associated protein 1 (YAP)